



**HAL**  
open science

# Assessment of asymmetrical rheological behavior of cementitious material for 3D printing application

Yohan Jacquet, Arnaud Perrot, Vincent Picandet

► **To cite this version:**

Yohan Jacquet, Arnaud Perrot, Vincent Picandet. Assessment of asymmetrical rheological behavior of cementitious material for 3D printing application. *Cement and Concrete Research*, 2021, 140, pp.106305 -. 10.1016/j.cemconres.2020.106305 . hal-03493635

**HAL Id: hal-03493635**

**<https://hal.science/hal-03493635>**

Submitted on 21 Nov 2022

**HAL** is a multi-disciplinary open access archive for the deposit and dissemination of scientific research documents, whether they are published or not. The documents may come from teaching and research institutions in France or abroad, or from public or private research centers.

L'archive ouverte pluridisciplinaire **HAL**, est destinée au dépôt et à la diffusion de documents scientifiques de niveau recherche, publiés ou non, émanant des établissements d'enseignement et de recherche français ou étrangers, des laboratoires publics ou privés.



Distributed under a Creative Commons Attribution - NonCommercial 4.0 International License

## Assessment of asymmetrical rheological behavior of cementitious material for 3D printing application

Yohan Jacquet<sup>1\*</sup>, Arnaud Perrot<sup>1</sup>, Vincent Picandet<sup>1</sup>

<sup>1</sup>University of South Brittany, UMR CNRS 6027, IRDL, 56100 Lorient, France

\*[yohan.jacquet@univ-ubs.fr](mailto:yohan.jacquet@univ-ubs.fr)

5

---

### Abstract

Among the multiplicity of construction methods based on digital  
concrete technologies, the most common one remains the extrusion-  
based process. Two opposed strategies have been developed in order to  
print a concrete structure using extrusion: the first one emphasizes the  
ease-of-pumping of material which is massively accelerated to ensure  
the stability of the structure, when leaving the extruder; the second one  
uses a firm mortar able to sustain the own weight of the structure during  
the printing, without requiring any accelerator. Both methods have their  
pros and cons and don't imply the same rheological requirements. Most  
of the recent literature assumes that both types of material (fluid and  
firm) follow the same trend of behavior and obey to the Von Mises  
plasticity criterion, while it has been demonstrated that firm cement-  
based materials can exhibit a pressure dependent behavior. Moreover,  
rheological study is mainly based on shear rheometry, while the  
extrusion-based printing process requires a description of the  
rheological behavior in compression to predict the global stability of  
the structure, and in tension to prevent cracks formation. This paper  
investigates the fresh behavior of cement paste and mortar under  
different solicitations (shear, compression, tension) for different water

15

20

25

Preprint submitted to Journal Cement and Concrete Research

to cement ratios. The analysis of these results allows to describe the transition between a ductile fluid material (symmetrical in tension and compression) that obeys to a Von Mises plasticity criterion, and a brittle and firm material (asymmetrical in tension and compression) that requires a pressure dependent plasticity criterion in order to predict its strength under a given solicitation.

Keywords: 3D printing, plasticity criterion, cementitious material, rheological behaviour: 00-01,99-00

## 1. Introduction

Today, the interest in digital concrete is increasing daily in the construction sector. This technological breakthrough is arising an ever-growing interest in digitally based fabrication technologies, divided in large families of techniques and adapted to an ever-increasing number of materials [1–6]. In this present study, we will focus on the printing of cement-based materials through the so-called extrusion-based process. In this way, the mechanical behavior of cementitious materials used in this process is described and characterized using new dedicated experiments. This extrusion-based process imposes that the fresh printed material exhibits some rheological requirements that allows for pumping, extrusion, shape retention and global stability of the structure [7–12]. Also, numerical simulations are being developed in order to predict the layer shape and cracks formation during the deposition process [13] for the sake of shape accuracy. All these conditions require a precise description of the behavior of the cementitious materials

under different nature of loading (tension for crack formation, compression for global stability, shear for pumping and self-bearing load ability, ...). For instance, during the deposition steps can induce a succession/combination of shearing, and bending with both tension and compression into the material. However, the description of the material behavior is almost carried out using shear rheometry and the Von Mises criterion is often assumed without experimental evidence as a plasticity criterion in order to link the measured shear yield stress, in pure shear state of stress, to the elongational one using the following and widely used relationship  $\sigma_c = \sqrt{3}\tau_c$  where  $\sigma_c$   $\sigma_0$  the elongational yield stress and  $\tau_c$  the shear yield stress. The Von Mises plasticity criterion also predicts that the strength of the material is the same in compression and in tension so that the behavior of the cementitious material can be qualified as symmetrical. Nevertheless, the Von Mises assumption can be questionable because it has been shown that cementitious materials containing a solid volume fraction higher than 80% of the random packing fraction can exhibit a frictional and dilatant pressure-dependent behavior [14–17]. A mechanical-oriented analysis on the extrusion-deposition process raised questions about fresh material behavior.

It is also important to keep in mind that the extrusion-based 3D printing process presents a variety of technological possibilities that ranges between two extreme cases [7]: the use of a fluid cementitious material that is easy to pump with the addition of hydration accelerator at the nozzle [18–20] in order to guaranty the global stability of the in-print structure on one side and the extrusion of a firm plastic cementitious materials that presents a yield stress higher than 1 kPa that can be

considered as “buildable” without the addition of accelerator [21,22].

80 The materials used in these two extreme cases are very different from a mechanical standpoint and it can be needed to highlight the difference in behavior between fluid or highly flowable and firm materials with high solid volume content cementitious pastes. Moreover, the boundary between this two materials is not so well clear-cut and a transition  
85 appears with increasing solid volume content as shown by Yammine et al. [17]. In order to describe this transition in behavior, the present paper studies the strength of cement paste and a mortar under different solicitations (tension, compression and shear) with varying water to cement mass ratio (W/C). Moreover, the type of mechanical behavior  
90 of cementitious materials can also evolved with hydration time. For example, a symmetrical Von Mises type self-compacting concrete begins to present an asymmetrical and dilatant behavior few hours after the contact between cement and water [23]. This will also be assessed by carrying rheological tests after different resting time.

95 This study proposes different types of characterization tests, either based on existing tests (squeeze flow, rotational rheometry), or other tests adapted from existing ones. The compression behavior of fresh cementitious materials is studied using both squeeze flow for firm materials [24–26] and slump test in elongational mode for the fluid  
100 ones [27]. The tensile yield stress will be assessed using gravity driven tensile test [28,29] for fluid materials, or a specific test especially developed in the frame of this research for firm pastes. Shear yield stress will also be assessed using common vane geometry. Tensile to compressive ratio assessment (i.e. symmetrical behavior) provides a

105 basis to discuss the adequacy between widely use Von Mises's  
plasticity criteria and material behavior in order to precisely model the  
process using, for instance, models implementation in numerical  
simulations. This study provides ranges of solid volume fraction where  
commonly used plasticity criteria can be used and where this kind of  
110 criteria are challenged and have to be replaced by a pressure-dependent  
one.

## 2. Materials and methods

### 2.1 Materials

Due to the multiplicity of mix designs developed for extrusion-based  
115 3D printing, this study proposes to focus on two very basic materials: a  
cement paste and a standard mortar. Both materials contain HRWRA  
(High Range Water Reducing admixture) at a dosage of HRWRA to  
cement mass ratio of 0.15%. Standardized sand is added to a sand to  
cement mass ratio of 3:1 in order to meet the requirement provided by  
120 EN 196-1 standard mortar. Information about the sand packing are  
obtained using a cylinder of 2 liters and a dedicated funnel. Random  
loose packing  $\phi_{rlp}$  and dense packing  $\phi_d$  (measured after a sample  
vibration lasting 1min) are measured after the filling of the testing  
cylinder :  $\phi_{rlp}=61.5\%$  and  $\phi_d=66.5\%$ . In the tested mortars, sand  
125 volume fractions range between 56.6% and 61.5% depending on the  
water to cement mass ratio. Cement paste and mortar mixes are  
prepared using a Warring blender and a Perrier mixer respectively.  
Water is firstly introduced in a bowl and then, premixed powders are

progressively added. After this first step of mixing at low velocity  
130 during 1 minute, a final step consisting in a high-speed mixing is  
performed during 3 minutes.

Parametric study about solid volume fraction is performed to set the  
water to cement ratios. Solid volume fraction ranges from 47.5% to  
58.8% for cement paste, and from 72.0% to 78.7% for standard mortar  
135 (i.e. effective water to cement ratios W/C are between 0.22 and 0.35 for  
cement paste, and between 0.39 and 0.56 for standard mortar). In order  
to perform mechanical characterizations under a similar state of  
structural build-up, all rheological measurements were carried out  
between seven and eight minutes after the first contact between water  
140 and cement.

## *2.2 Shear yield stress measurement*

Each mix design is characterized using shear yield stress measurements  
in order to evaluate the possible deviation between symmetric plasticity  
criterion (e.g. Tresca or Von Mises criterion) and the observed material  
145 behavior. Anton Paar MCR 702 rheometer equipped with a vane  
geometry is used in this study. Shear test device consists of a four-  
bladed vane tool geometry ST22-4V-40 (40 mm high and 22 mm in  
diameter) and a PETG printed cup to provide a 1.75mm gap width. 3D  
printed cup's wall presents a roughened surface to avoid wall slip.

150 A reproducible method has been developed to characterize shear  
behavior from the more fluid to the firmest material allowing to  
minimize the effects of the material stress history. Shear rheological  
measurements consist in two steps: first, a Small Amplitude Oscillatory

155 Shear (SAOS) test is performed to reach a steady state regime at a  
determined strain amplitude belonging to the Linear Visco-Elastic  
Region (LVER). Considering the whole solid volume fraction range  
selected in this study, a strain amplitude of 0.01% is set to stay with  
linear viscoelastic behavior, according to preliminary amplitude sweep  
test and in agreement with recent literature [30–33]. When steady state  
160 regime is achieved, continuous shear test is carried out at a defined  
shear rate between  $0.005\text{s}^{-1}$  and  $1\text{s}^{-1}$ . By plotting shear stress - shear rate  
curve, Herschel Buckley law parameters can be determined for each  
mix design according to  $\tau = \tau_c + k \dot{\gamma}^n$ . Where  $k$  is the material  
consistency and  $n$  the flow index.

### 165 2.3 Characterization of compressive behaviour

#### 2.3.1 Uniaxial compression test for firm materials -or Squeeze Flow test

Characterization of the behavior of firm materials under uniaxial  
compression loading has become a usual test since the development of  
3D printing of concrete [8,34]. This description is required in order to  
170 predict one of the failure mode of the in-print structure which is due to  
the plastic collapse of the first layer and the ability of the fresh printed  
structure to sustain its own weight: the so-called buildability [35].

Squeeze Flow [Figure 1(a)] test consists in a uniaxial compression  
loading of a sample with a 2:1 aspect ratio between two parallel  
175 lubricated plates performed at controlled displacement rate. The chosen  
slenderness allows to avoid particle size effects and promote a diagonal  
shear failure [12,34]. Test is performed at an axial velocity of  $0.1\text{ mm.s}^{-1}$

<sup>1</sup> in order to consider quasi-static conditions. For significant deformations, dimensions of the sample can be updated in the compression stress computation, considering a diameter that continuously increases with the displacement of the upper plate, as long as the continuity of material can be assumed.

The compression yield stress (or compression strength)  $\sigma_{c,u}$  is defined as the ratio the maximum recorded force  $F_{max}$  to the updated diameter of the sample.

### 2.3.2 Compression test for fluid materials -or Slump flow test

For fluid materials, it is not possible to prepare self-standing samples: using uniaxial compression test is therefore not possible. An alternative way to estimate the compressive strength of the material is to adapt slump flow by generating purely elongational flow as proposed by Roussel and Coussot [27].

Slump test is a common method used to characterize ordinary cement-based materials workability [27,36,37]. Originally developed for concrete, this method has been extended to mortar and cement paste to determine yield criterion using mini-cone geometry [38,39].

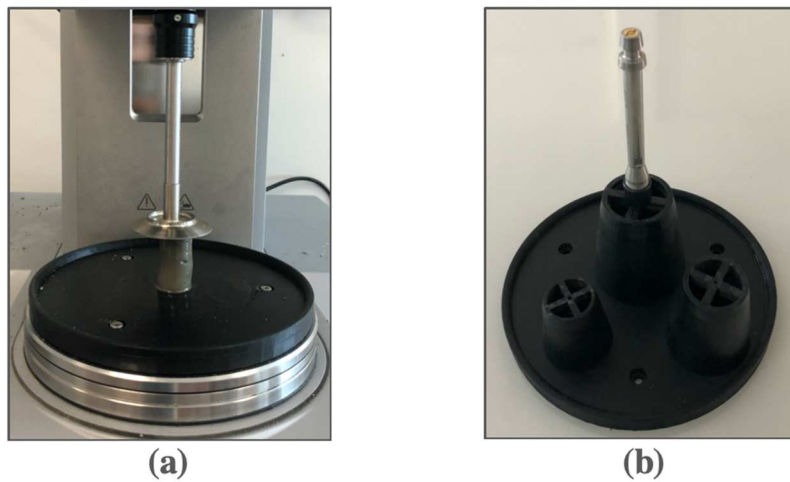
It is interesting to note that for small slump ratio (final to initial height of the sample), the slump test induces an elongational flow that allows the estimation of the elongational yield stress of the material that can be assimilated to its compressive strength [27]. The elongational yield stress can be computed by writing a stress balance equation between gravity and material compressive strength. In such case, deviatoric terms of stress tensor due to material spreading is negligible compared

to the hydrostatic terms induced by gravity, whatever the volume of the sample.

205 As a consequence, in this study, volume and dimensions of the cone are chosen to meet the geometrical conditions required to induce such purely elongational flow. To do this, different cone geometries are proposed in Table 1. This type of mechanical self-compression test leads to a final height  $S$  under material's own weight. Considering  
210 material density and gravity, the ultimate compressive stress can be determined according to  $\sigma_{c,u} = \rho g S$ .

The cones and the plate [Figure 1(b)] are 3D printed with ABS and put on MCR-702 using SCF-7 tool connected to 50 N load cell that controls cone lifting operation in order to increase test reproducibility. All  
215 contact areas are highly lubricated using Teflon<sup>®</sup> grease. Material is first introduced inside the cone and slump test is performed at a lifting speed of  $0.1 \text{ mm.s}^{-1}$  to remain in quasi-static conditions and in order to minimize viscous effects. The right dimension of the cone to minimize shear effects has to be set. Some preliminary tests consist in random  
220 tests of materials with different W/C ratios to reach a slump value around a predefined range of validity of the elongational flow assumption associated to the height of the cone. Ability of the geometry to accurately measure the compressive strength is linked to the minimization of shear effects. According to the work of Roussel and  
225 Coussot [27], the shear effects are almost negligible for a ratio between slump and initial height lower than 25%. Considering all cone geometries, this criterion can be re-written as a ratio between initial lower cone radius  $R_{\text{max}}$  (see Table 1) and the final re-calculated radius

230 triggered by material spread  $R_{\text{spread}}$  considering sample volume stability. Below criterion values  $R_{\text{max}}/R_{\text{spread}}$  of 0.8, the size of the cone has to be reduced. Geometries used in this study are listed in Table 1.



235 **Figure 1** Devices used to characterize compressive strength of cement-based materials -- (a) Squeeze flow test performed on a 2:1 sample using Anton Paar MCR 702 (b) Cones with various height used to performed gravity driven Slump test in elongation mode. The cone is attached to the MCR 702 which lift the device at a constant velocity.

240 **Table 1** Cone geometries for Gravity Driven Slump test (see Figure 1(b))

Cone	Abrams cone	1 <sup>rst</sup> cone	paste cone	2 <sup>nd</sup> paste cone	3 <sup>rd</sup> paste cone
$H_0$ [mm]	300	50		40	30
$R_{\text{min}}$ [mm]	100	35		28	21
$R_{\text{max}}$ [mm]	200	50		40	30

## 2.4 Characterization of tensile behaviour

### 2.4.1 Tensile test for firm materials -or Double Dumbbell Device test

The development of this tensile test was imagined from conventional  
245 testing procedure used for high strength materials such as steel and  
hardened concrete and designed to take advantages of the existence of  
the material self-standing properties. The lower solid volume fraction  
materials can easily be tested using capillary rheometers but beyond a  
certain concentration of particles, structuration phenomena can occur in  
250 the extruder (e.g., consolidation or compaction and drainage) [40]. This  
test is presented here as a solution to evaluate tensile yield stress (or  
tensile strength) of firm cementitious materials at fresh state, which  
have a high enough yield stress to ensure stability inside the dumbbell-  
shape specimens.

255 Double Dumbbell Device tensile test consists of upper and lower  
brackets, and of two exchangeable dumbbells secured by a clamping  
ring. The device is mounted on the Anton Paar MCR-702 rheometer  
using SCF-7 tool to connect the upper bracket to the 50N load cell.  
Once the assembly of the double dumbbell assembly is set in the  
260 brackets, clamping ring is carefully removed and then, test can be  
performed at an axial velocity of  $0.1\text{mm}\cdot\text{s}^{-1}$ . Tensile elastic domain of  
cement-based materials is very small: that's why an initial value of  
normal force shall be reported and an acquisition frequency has to be  
set above a minimal value of 2 Hz.

265 The tensile strength of the tested material  $\sigma_{t,u}$  is computed from the  
ratio of the maximum recorded force to the initial material section.

#### 2.4.2 Tensile test for fluid materials -or Gravity Driven Tensile test

Gravity Driven tensile test consists of a 5 cm diameter extruder fitted with a PTFE piston, placed on a metal frame. The extruder is filled with fresh material and pushed through a 14 mm nozzle diameter. The device is placed on a compressive machine to control displacement of the piston, and thus the flow rate of material. Numerical method based on video analysis allows to check the linearity of the flow. Considering the ratio of the reduction of the extruder section and the piston velocity,  $v_{piston}$ , the extrudates displacement rate,  $v_{sample}$ , is given by  $v_{sample} = v_{piston} \cdot \frac{D_{piston}^2}{D_{die}^2}$ . The piston velocity is set to 0.25 mm.s<sup>-1</sup> and the axial force is recorded using a 5 kN load cell.

A previous study has shown that such low piston velocity minimizes the scattering of the results obtained with Double Dumbbell Device test [29]; At such velocity, quasi-static conditions can be considered and viscous effect can be ignored.



**Figure 2** Devices used to characterize tensile behavior of cement-based materials -  
 - (a) Double Dumbbell Device attached to the MCR 702 rheometer (b) Gravity  
 Driven Tensile test using a cylindrical piston extruder.

285

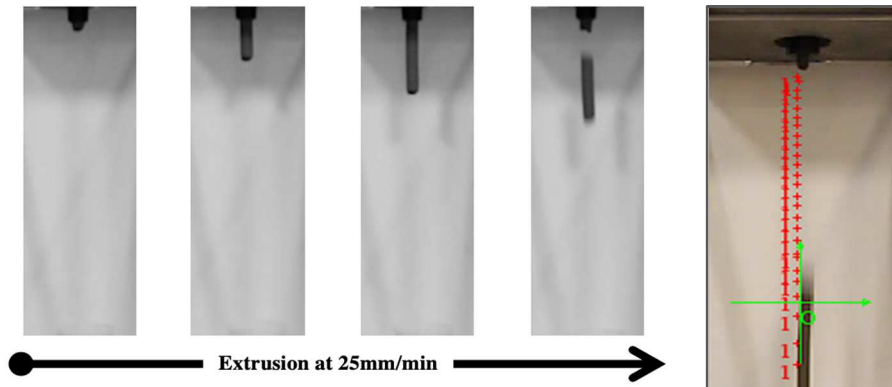


**Figure 3** Gravity Driven tensile test on standard mortar at 25mm/min piston velocity  
 and sample length measurement by video analysis.

290

The gravity drives the failure of the material allowing to determine the  
 tensile yield stress or tensile strength of material by weighing broken  
 samples. Weighting of the “so-called” slug [28] at least five times to  
 ensure a proper mean value and its associated standard deviation. In  
 addition, to check the linearity of the flow, digital scoring [Figure 3]

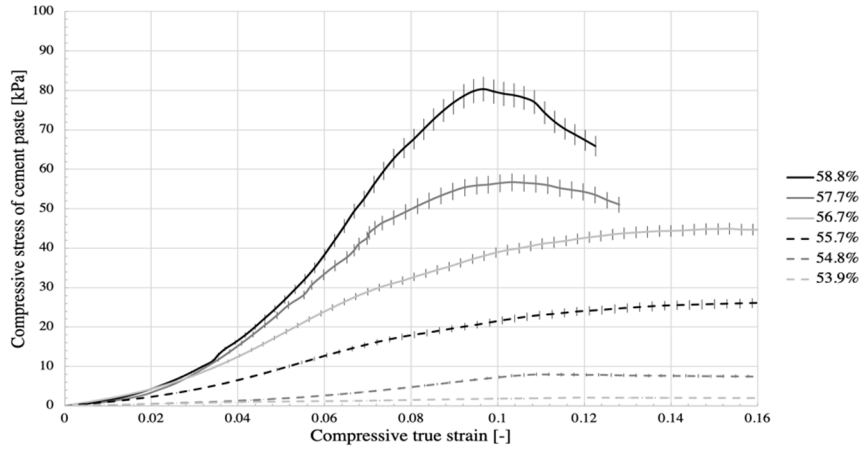
based on a video recording can be used to compute the length of the  
295 sample at the time of failure. Considering the deviation of material  
density, the tensile strength of material can be assessed assuming  $\sigma_{t,u} =$   
 $\rho g L_{sample}$ . The steady state of the flow must be reached before  
picking up and weighing extruded so-called “slugs”.

### 3. Experimental results and discussion

#### 300 3.1 Comparative study of tensile and compressive material's behaviours at fresh state

Choosing the right characterization method is essential to adequately  
test all materials with varying W/C ratios. Whether in tension or in  
compression, each device has some physically-based limitations,  
305 directly correlated to the stability of material under the effects of  
gravity: a transition area can be observed wherein both testing devices  
can be used. It is interesting to note that both testing methods can be  
used in the shear stress range between 0.5 to 1kPa.

The compressive behavior is characterized either using Squeeze Flow  
310 test (see Figure 4 and 5) for firm materials, or Gravity Driven Slump  
test in pure elongation mode for the most fluid ones. The  
characterization of tensile behavior is performed using Double  
Dumbbell Device (see Figure 6 and 7) for the firmest materials, and a  
Gravity Driven tensile test for the most fluid ones. Each deviation value  
315 is reported on graphs for each measurement: it is interesting to notice  
that the deviation of Squeeze Flow results increases as well as W/C  
decreases due to appearance of internal friction.



320 **Figure 4** Compression Squeeze Flow (SF) tests performed on cement pastes.

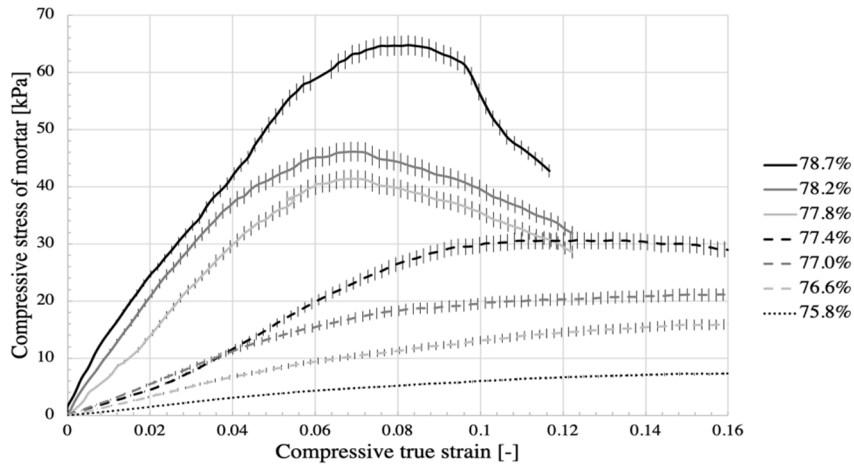


**Figure 5** Compression Squeeze Flow (SF) tests performed on standard mortars.

325 In figure 4 and 5, it can be noticed that the material apparent rigidity tends to increase as solid volume fraction is increasing (or with decreasing water to cement ratio) which is in agreement with common literature [41]. Moreover, a continuous transition of behavior can be

observed from the lowest volume fraction to the highest one: while a  
330 stress plateau is observed for the lowest water to cement ratios. Stress  
peaks are observed for the other tested materials. It is interesting to note  
that this peak appears more pronounced and at a strain value that  
decreases with the solid content. This shows the transition between a  
ductile flowing material to a quasi-solid dilatant and brittle one. Also,  
335 the compressive apparent rigidity appears higher for the mortar than for  
the corresponding cement paste. This is in agreement with theoretical  
modeling developed by Mahaut et al. [42]. The mortar presents a more  
brittle behavior than the cement paste, due to the presence of sand  
particles.

340 A deeper analysis of the stress-strain curve of cement paste (Figure 4)  
highlights two different elastoplastic phases: the first, which induces  
breakings of the early hydrates characterized by a weak chemical  
bonding; the second, reached over a kind of plateau value, exhibits a  
more rigid behavior because of the high concentration of Calcium  
345 Silicate Hydrates covalent bonds. This observation is in agreement with  
the conclusions of Roussel et al. and Ma et al. [30,33].

The analysis of the curves obtained in tension (Figure 6 and 7) globally  
confirms the conclusions drawn from compression test results. Note  
that for higher W/C ratio, stress vs. strain cannot be obtained from  
350 gravity driven slump flow and self-tensile tests.

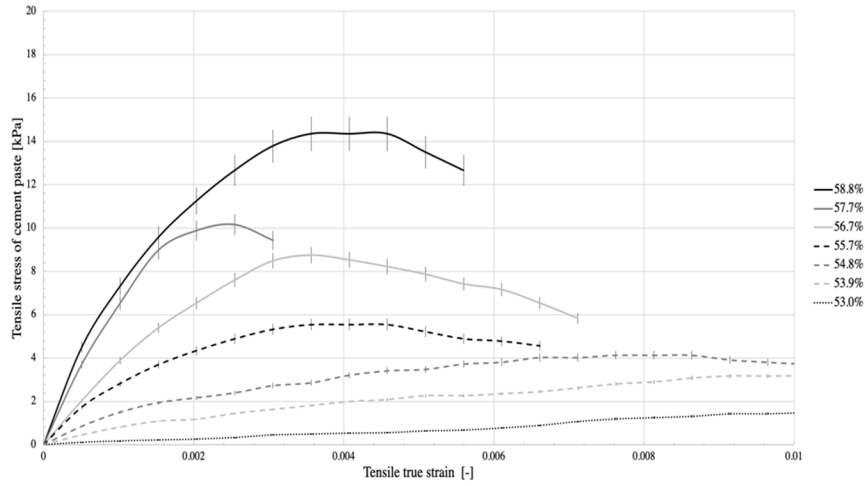


**Figure 6** Double Dumbbell Device (3D) tensile tests performed on cement pastes.

355

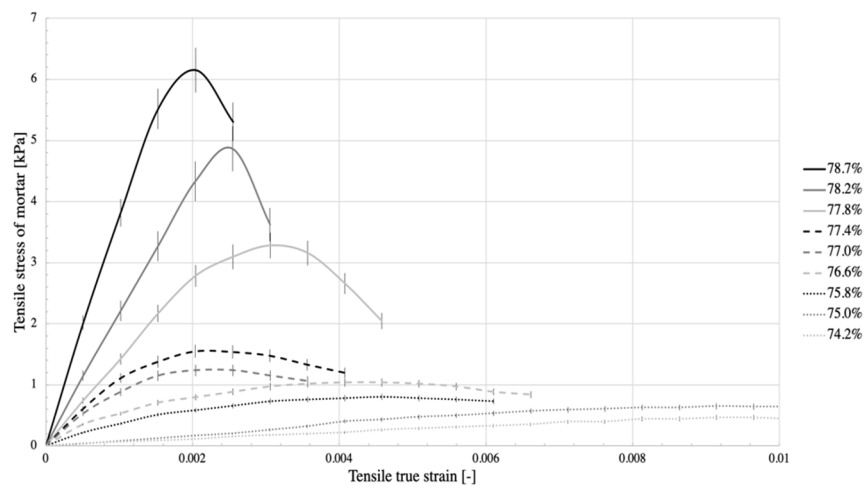


**Figure 7** Double Dumbbell Device (3D) tensile test performed on standard mortars

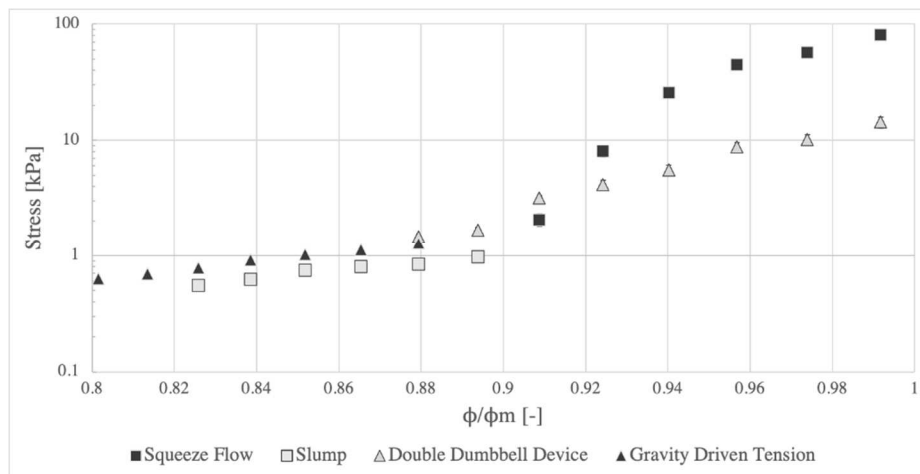
360 In figure 8 and 9, the measured tensile and compressive strengths obtained from the four measurement techniques are plotted in function of the solid volume content for cement paste and mortar respectively. It allows to assess the difference between tensile and compressive

strengths and to verify the symmetry of the uniaxial mechanical behavior of the material. An interpretation of these measurements highlights a similar behavior for both materials: fluid materials have a substantially symmetrical behavior because tensile and compressive strength follow the same trend and shows very close values for the same solid volume fraction. However, over a critical solid volume content of 0.53 for cement paste (i.e around 90% of the maximum packing fraction) and 0.75 for standard mortar (equivalent to W/C=0.28 for cement paste, and W/C=0.48 for standard mortar), a clear distinction appears between the tensile and the compressive behavior. The material starts to exhibit an asymmetrical behavior. It can be interesting to note that this change occurs for material tensile strength of few kPas. This is in agreement with the apparition of a frictional, dilatant and pressure dependent behavior during the early hydration of SCC as described by Mettler et al. [23]. Over this critical solid fraction, the asymmetry increases gradually.

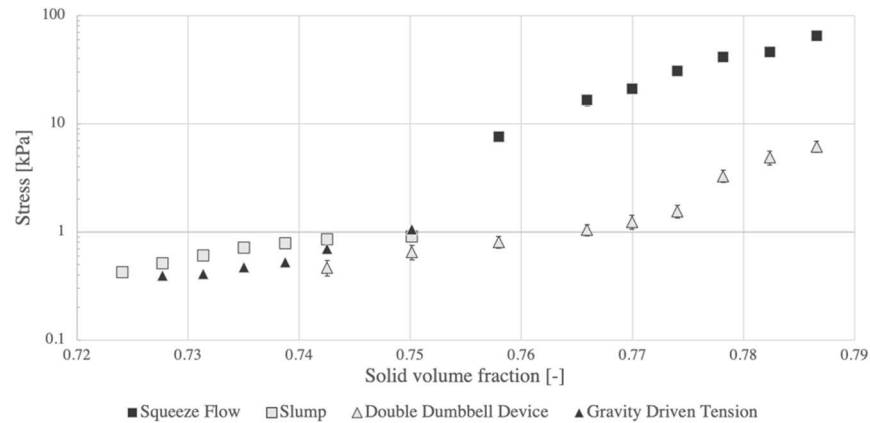
It is also interesting to note that plotted curves are S-shaped which is an evidence of the transition from colloidal hydrodynamic interaction driven flow to a dilatant flow driven by direct contacts [16,17]. It is interesting to note that the behavior of the mortar appears more rigid and more brittle than the cement paste. Such behavior is highlighted by the sharper stress peak occurring for mortar (Figure 5 and 7), and by the lower range of strain values measured at the failure, for cement pastes (Figure 4 and 6). This can be explained by the macroscopic strain applied to the mortar concentrates between the non-deformable sand grains. The matrix is therefore submitted to higher strains than the

macroscopic ones and failure is therefore reached for lower  
390 macroscopic strains.

For mortar and below the critical solid volume fraction, a small but  
noticeable difference between tensile and compressive strength can be  
attributed to the fact that sand particles don't contribute to the material  
395 tensile strength as discussed in the next section.



400 **Figure 8** Comparison of compressive and tensile strengths of cement paste in function of solid volume fraction vs. maximum solid volume fraction. Square dots show compressive strength while triangle dots show tensile strength ( $\Phi_m=0.59$ ).



405 **Figure 9** Comparison of compressive and tensile strength of mortar in function of solid volume fraction. Square dots show compressive strength while triangle dots show tensile strength.

### 3.2 The widely used Von Mises plasticity criterion challenged

Tensile and compressive measurements have shown that material having a strength under around 2 kPa, or solid volume fraction lower than a critical value, can be considered as symmetrical: for this range of  
 410 W/C, the Von Mises plasticity criterion provides an enough accurate result. When the solid volume fraction increases, the asymmetry appears, and thus the validity of Von Mises' criterion is challenged.

415 To further discuss the validity of Von Mises plasticity criterion, static shear test measurements are performed using vane geometries on cement paste (Figure 10) and mortar (Figure 11). Further clarifications may be given for materials with the higher solid volume fraction, showing the large variations in results due to larger internal friction  
 420 effect.

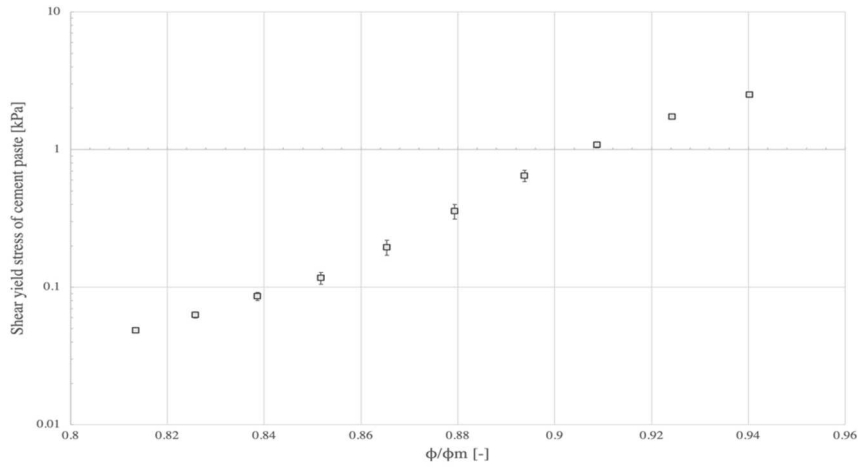
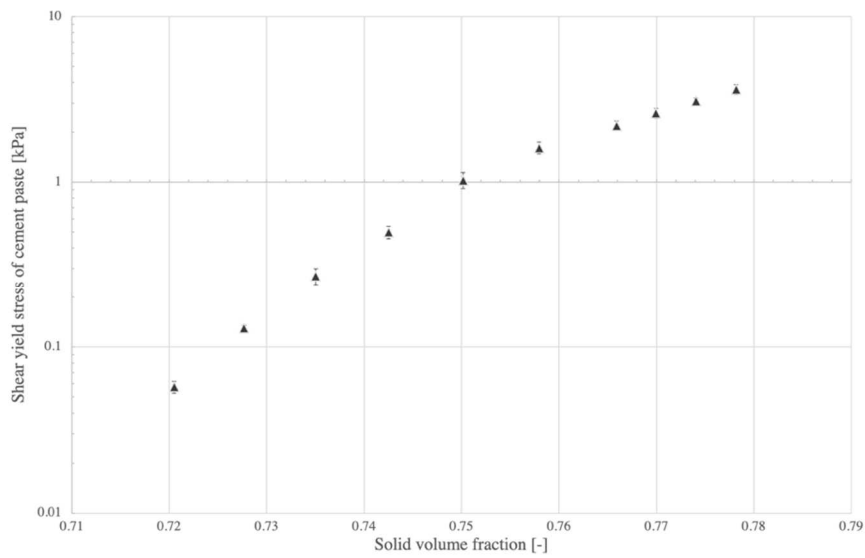


**Figure 10** Shear characterization of cement paste with  $\Phi_m=0.59$ . Evolution of static yield stress in function of the dimensionless solid volume fraction.

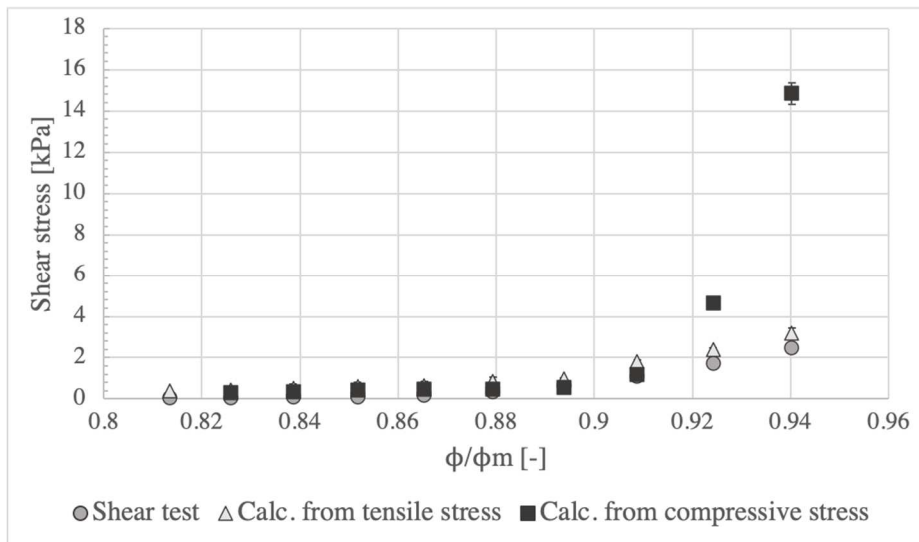


425

**Figure 11** Shear characterization of standard mortar. Evolution of the static yield stress in function of the solid volume fraction.

For a pure shear stress state (as assumed in vane test), shear yield stress values  $\tau_c$  allow to estimate a Von Mises tensile  $\sigma_{y,t}$  and  
 430 compressive  $\sigma_{y,c}$  equivalent yield stresses according to the following

equation  $\sigma_{y,\alpha} = \tau_c \cdot \sqrt{3}$ . These values are plotted in figure 12 and 13 and compared with compressive and tensile strength measurement of cement paste and standard mortar reported in Figures 8 and 9.



435

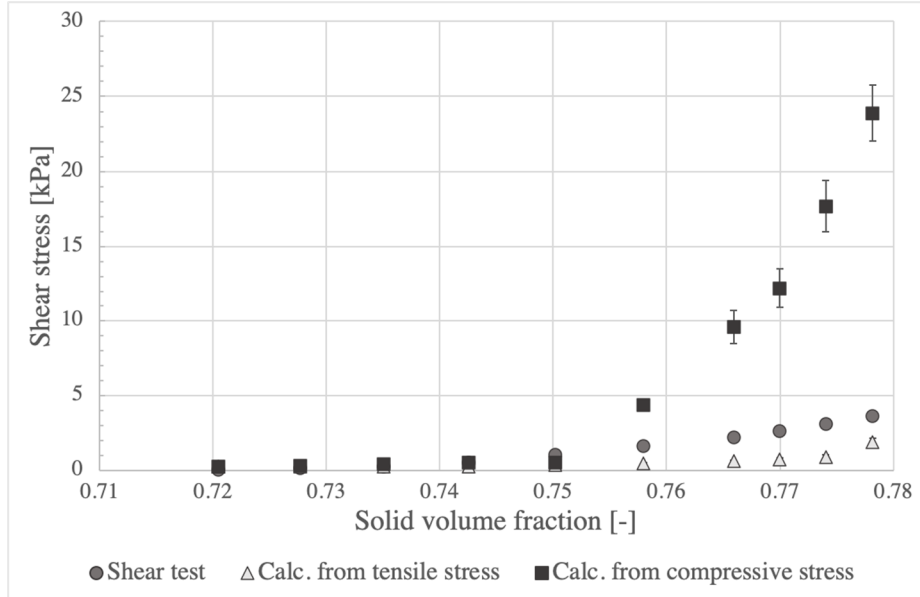
**Figure 12** Comparison between calculated Von Mises equivalent stresses and static shear measurements (case of **cement paste**) with  $\Phi_m=0.59$

440 For cement paste (Figure 12), The equivalent stress values obtained from shear strength measurements follows exactly the same trend as tensile strength with various solid volume fractions. As previously observed, the equivalent stress and compressive strength are below 2 kPa with a critical solid volume fraction of 0.54 before divergence. It clearly shows that the Von Mises plasticity criterion cannot be used in order to study the stability of in-print structures for such firm and high yield stress materials and that computing the compressive yield stress from static shear yield stress measurement can be misleading. This can

445

explain why some authors have used pressure dependent plasticity criterion such as the Coulomb criterion in order to study the global shape stability of a structure printed using a firm concrete [12,43].  
450

For mortar (Figure 13), the behavior appears more complex. If the comparison between equivalent stress and compressive behavior allows to draw the same conclusion on the domain of validity of the Von Mises criterion, the comparison between equivalent stress computed from shear measurements and tensile strength is rather different than  
455 for cement paste. In the case of mortar, the tensile strength appears lower than the equivalent stress. It has been shown that the addition of solid inclusions such as sand particles increases the shear yield stress of cement paste [15,42]. Also, coarse aggregates added to mix designs  
460 allows to minimize the material cost and, with a well-defined mix design, allow to reach good mechanical performances at the hardened state. However, solid inclusions weaken the material in tension because they have any cohesion between each other while cohesion with cement particles is weak. Basically, the addition of sand reduces the material section that can actively resist in tension. Another significant aspect,  
465 directly linked to the mix design, can be considered to explain tensile behavior and fracture occurrence: air entrained due to mixing and material defaults induced by the interface between inclusions. Such discontinuities can drive the tensile failure and can be responsible for fracture localization and initiation. Further studies could consist in a  
470 statistical analysis of air influence on the tensile behavior which may be impacted by the air content and bubbles size distribution.



475 **Figure 13** Comparison between calculated Von Mises equivalent stresses and static shear measurements (case of **standard mortar**)

It can be interesting to study the contribution of cement paste to the material tensile strength. By making a distinction between the solid volume fraction of cement and the solid volume fraction of sand, the effective contribution of cement paste to the material tensile strength

480 can be estimated assuming that sand does not play any role in tension. The measured tensile strength of standard mortar,  $\sigma_{t,u}$ , are computed from the total section of the sample  $S_{total}$ :  $\sigma_{t,u} = \frac{F}{S_{total}}$ . However, if we

consider in a first approach that only the cement paste opposes tensile loading, it can be interesting to correct this value by taking into account

485 only the cement paste section:  $\sigma_{t,paste} = \frac{F}{S_{paste}} = \frac{F}{(1-\varphi_{sand}) \cdot S_{total}}$  where

$\varphi_{sand}$  is the solid volume fraction of standard sand. An updated strength value can be determined and expressed as follow:  $\sigma_{t,paste} = \frac{\sigma_{t,u}}{(1-\varphi_{sand})}$ .

This estimation of cement paste contribution on mortar strength can be  
490 plotted on Figure 14.

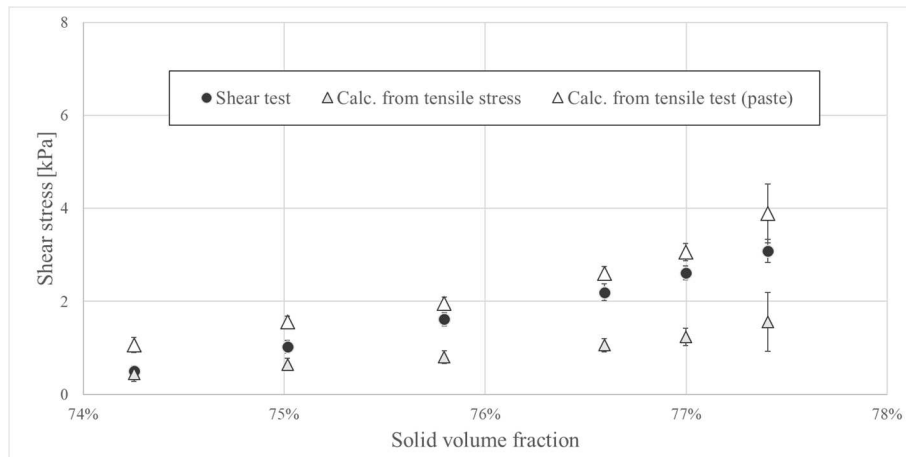


**Figure 14** Assessment of contribution of cement paste to the cohesion  
495 of mortar by comparing calculated von Mises equivalent stresses within  
cement pastes and measured shear stress.

As a first approach, it can be seen that the updated equivalent stress  
computed from tensile test are close to the shear stress showing that  
500 sand particles in fresh mixes have no mechanical contribution in  
tension. This type of behavior increases the asymmetrical behavior of  
the material and can be detrimental to the process, due to the increased  
risk of induced cracks if this phenomenon is not taken into account. For  
instance, additive manufacturing by extrusion-deposition process of  
505 firm cement-based materials can involves bending stress if the layer  
undergoes a free deposition process (i.e. the material lace leaves the  
nozzle and only gravity makes it fall over the previously deposited  
later). In this case, compressive and tensile asymmetrical behavior can

lead to the occurrence of cracks or micro-cracks into the tensioned  
510 section of the printed layers. One solution to prevent such formation  
can be to mix-designed cementitious materials with a lower solid  
volume fraction in order to reduce the material asymmetrical behavior.  
When material is designed with a high shear yield stress value, its  
strength under its own weight is preferred to its extrudability, and thus  
515 to its bending ability. Therefore, a significant consequence can be  
cracks formation, induced by the asymmetrical behavior, leading to  
potential durability concerns of hardened concrete, or accelerated  
leaching in case of underwater printing [44].

### 3.3 *Evolution of tensile and compressive strength with cement* 520 *hydration*

With resting time and early hydrates formation, cementitious material  
undergoes a structural build-up. Early hydration process implies  
microstructural changes that increases its strength and begins its  
transition toward brittle hardened concrete. In order to take this material  
525 strengthening into account, authors have proposed different models to  
predict the global stability of the in-print structures that describes the  
increase in the static shear yield stress of cementitious materials with  
resting time [8,30,45–48]. However, those models does not account for  
the transition toward a pressure dependent behavior as observed by  
530 Mettler et al. [23]. Therefore, it can be needed to separately describe the  
evolution of both compressive and tensile strength of cementitious  
materials.

In order to assess the tensile and compressive strength evolution at very early age, measurements are carried out periodically until 5h30 hydration time. The choice of tested material is made to start the analysis on a fluid mortar with a water to cement ratio of 0.50 that initially presents a Von Mises behavior type. Exchangeable Double Dumbbell Devices (see Figure 15) are filled with this material and stored in a controlled atmosphere to avoid desiccation. The same procedure is followed for compression samples using 2 cm diameter samples with a 2:1 slenderness.



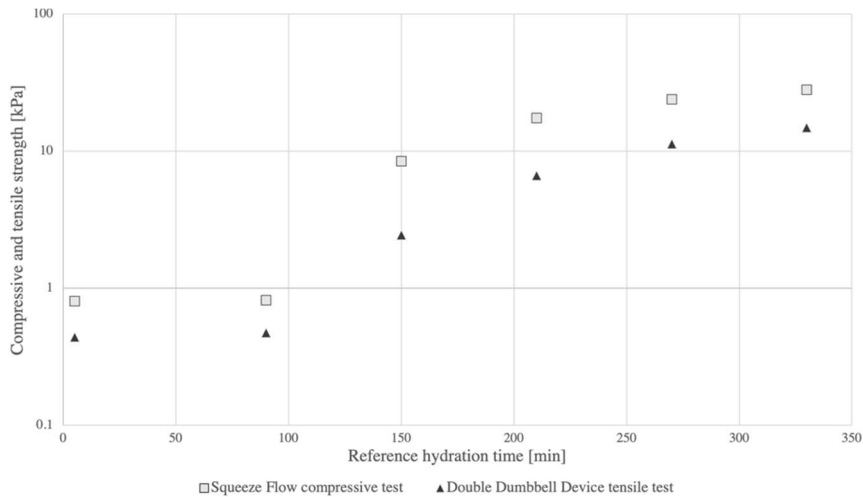
**Figure 15** Exchangeable part of Double Dumbbell device filled with mortar at rest before tensile strength measurements.

545

It should be noted that the first obtained values for each type of solicitation (in tension and in compression), at 10 minutes after the contact between cement and water, are determined using gravity driven tensile test and squeeze flow test respectively due to material initial fluidity.

550

Then, approximately every one hour, compressive and tensile measurements are performed using developed procedure for firm materials and their respective values are plotted in Figure 16.



555

**Figure 16** Compressive and tensile strength measurements during cement hydration

It can be seen in figure 16 that the first measurement shows that the compressive strength and the tensile strength are close, even if the compressive strength is slightly higher because of the non-cohesive nature of sand particles as explained in section 3.2. Asymmetrical behavior phenomenon already occurs and is magnified with hydration time, especially after 90 minutes due to the appearance of pressure-dependent behavior. At rest, without any interaction, material tends to reach an equilibrium solid state. As hardened concrete would, material seems to exhibit a continuous increase in compressive to tensile strength ratio relative to its asymmetrical behavior.

Such transition in the behavior of the mortar from symmetrical to asymmetrical cannot be explained by an increase in solid volume fraction that is sufficient to overcome a critical value like in figure 8 and 9. In the range of investigated paste age, Mantelatto et al. [47,49]

570

have shown that the shear yield stress exponential increase (responsible for material flow loss) after the linear evolution proposed by Roussel [48] cannot be explained by a significant increase of the solid volume fraction. The authors show that there is a close relationship between the instantaneous specific surface due to the hydrates creation and the materials shear static yield stress. The authors explain that newly forms hydrates can fix part of superplasticizer and decrease its efficiency but more certainly can create an entangled and jammed network that can change the type of mechanical behavior of the cementitious material.

Therefore, the occurrence of the asymmetrical behavior can be induced by either an initial solid volume fraction higher to a critical value making the material having a granular like behavior or by the creation of an entangled network of early hydrates formed few hours after the cement/water contact. It is important to note that asymmetrical behavior appears in the second case even if the solid volume fraction remains lower than the critical value responsible for the granular case.

This clearly shows that the Von Mises criterion cannot be used for long lasting printing process even if the initial rheological behavior of the cementitious materials presents low yield stress values. It means that shear rheometry is not sufficient to fully describe the evolution of the mechanical behavior at early age for 3D printing applications.

#### **4. Conclusion**

This study details experimental methods for the determination of the tensile and compressive behavior of cement-based materials at fresh state. Uniaxial compression tests also called squeeze flow tests are used

to assess the compressive behavior of firm material and for the most fluid materials. When it is not possible to prepare a self-standing samples, a method based on slump test in pure elongation mode has  
600 been adapted to ensure quasi-static conditions by controlling the axial displacement at a low speed rate using the axial motor of a rheometer.

Newer characterization methods have been developed to determine the tensile strength of cement-based materials. An innovative device  
605 consisting in double dumbbell device has been used when the material is firm enough to not flow under its own weight. For the most fluid ones, inspired by capillary rheometer, a gravity driven tensile test device has been developed.

Once protocols of the different characterization tests have been defined  
610 to assess mechanical tensile and compressive behavior, measurements are performed on cement paste and EN 196-1 standard mortar. If the tested materials show a Von Mises type plastic criterion under a critical solid volume fraction and shear yield stress value of around 2 kPa, an asymmetrical pressure dependent behavior has been highlighted for  
615 higher solid volume fractions or after a sufficient structural build-up due to cement early hydration. This asymmetrical behavior raises the issue of the overused Von Mises criterion for FEM numerical methods and analytical prediction tools when studied materials exhibit yield stress higher than few kPas. A deeper compressive to tensile behavior  
620 analysis shows that, beyond a given threshold, the tensile behavior is linearly linked to shear stress, as the compressive one diverges: granular pressure dependent aspects of material have to be considered. This phenomenon starts the development of an asymmetrical

mechanical behavior that ends into weaker stiffness and strength in  
625 tension than in compression, as hardened concrete is already described  
for more than a century.

It has also been shown that sand particles in mortars leads to a  
weakening of the material in tension, in comparison of shear or  
compression resistance, due to their non-cohesive nature. Therefore, it  
630 seems that aggregates addition magnifies the behavior asymmetry,  
creating an inherent inequality between tensile and compression  
strengths of the fresh material.

## References

- 635 [1] R.A. Buswell, W.R.L. da Silva, F.P. Bos, H.R. Schipper, D. Lowke, N. Hack, H. Kloft, V. Mechtcherine, T. Wangler, N. Roussel, A process classification framework for defining and describing Digital Fabrication with Concrete, *Cement and Concrete Research*. 134 (2020) 106068. <https://doi.org/10.1016/j.cemconres.2020.106068>.
- 640 [2] V.S. Fratello, R. Rael, Innovating materials for large scale additive manufacturing: Salt, soil, cement and chardonnay, *Cement and Concrete Research*. 134 (2020) 106097. <https://doi.org/10.1016/j.cemconres.2020.106097>.
- [3] M.S. Khan, F. Sanchez, H. Zhou, 3-D printing of concrete: Beyond horizons, *Cement and Concrete Research*. 133 (2020) 106070. <https://doi.org/10.1016/j.cemconres.2020.106070>.
- 645 [4] E. Lloret-Fritschi, T. Wangler, L. Gebhard, J. Mata-Falcón, S. Mantellato, F. Scotto, J. Burger, A. Szabo, N. Ruffray, L. Reiter, F. Boscaro, W. Kaufmann, M. Kohler, F. Gramazio, R. Flatt, From Smart Dynamic Casting to a growing family of Digital Casting Systems, *Cement and Concrete Research*. 134 (2020) 106071. <https://doi.org/10.1016/j.cemconres.2020.106071>.
- 650 [5] D. Lowke, E. Dini, A. Perrot, D. Weger, C. Gehlen, B. Dillenburger, Particle-bed 3D printing in concrete construction – Possibilities and challenges, *Cement and Concrete Research*. (2018). <https://doi.org/10.1016/j.cemconres.2018.05.018>.
- 655 [6] A. Perrot, *3D Printing of Concrete: State of the Art and Challenges of the Digital Construction Revolution*, Wiley-ISTE, 2019.
- [7] V. Mechtcherine, F.P. Bos, A. Perrot, W.R.L. da Silva, V.N. Nerella, S. Fataei, R.J.M. Wolfs, M. Sonebi, N. Roussel, Extrusion-based additive manufacturing with cement-based materials – Production steps, processes, and their underlying

- 660 physics: A review, *Cement and Concrete Research*. 132 (2020) 106037.  
<https://doi.org/10.1016/j.cemconres.2020.106037>.
- [8] A. Perrot, D. Rangeard, A. Pierre, Structural built-up of cement-based materials used for 3D-printing extrusion techniques, *Materials and Structures*. 49 (2016) 1213–1220.
- 665 [9] N. Roussel, Rheological requirements for printable concretes, *Cement and Concrete Research*. (2018). <https://doi.org/10.1016/j.cemconres.2018.04.005>.
- [10] A.S.J. Suiker, R.J.M. Wolfs, S.M. Lucas, T.A.M. Salet, Elastic buckling and plastic collapse during 3D concrete printing, *Cement and Concrete Research*. 135 (2020) 106016. <https://doi.org/10.1016/j.cemconres.2020.106016>.
- 670 [11] T. Wangler, E. Lloret, L. Reiter, N. Hack, F. Gramazio, M. Kohler, M. Bernhard, B. Dillenburger, J. Buchli, N. Roussel, R. Flatt, Digital Concrete: Opportunities and Challenges, *RILEM Technical Letters; Vol 1* (2016)DO - 10.21809/Rilemtechlett.2016.16. (2016).  
<https://letters.rilem.net/index.php/rilem/article/view/16>.
- 675 [12] R.J.M. Wolfs, F.P. Bos, T.A.M. Salet, Early age mechanical behaviour of 3D printed concrete: Numerical modelling and experimental testing, *Cement and Concrete Research*. 106 (2018) 103–116.  
<https://doi.org/10.1016/j.cemconres.2018.02.001>.
- [13] R. Comminal, W.R.L. da Silva, T.J. Andersen, H. Stang, J. Spangenberg, Influence of Processing Parameters on the Layer Geometry in 3D Concrete Printing: Experiments and Modelling, in: *RILEM International Conference on Concrete and Digital Fabrication*, Springer, 2020: pp. 852–862.
- 680 [14] T. Craipeau, Y. Jacquet, T. Lecompte, F. Toussaint, A. Perrot, Characterization of the shear behavior of mineral suspensions at controlled negative pressure conditions, *Powder Technology*. 364 (2020) 60–69.  
<https://doi.org/10.1016/j.powtec.2020.01.042>.
- 685 [15] T. Lecompte, A. Perrot, V. Picandet, H. Bellegou, S. Amziane, Cement-based mixes: shearing properties and pore pressure, *Cement and Concrete Research*. 42 (2012) 139–147.
- 690 [16] N. Roussel, A. Lemaître, R.J. Flatt, P. Coussot, Steady state flow of cement suspensions: A micromechanical state of the art, *Cement and Concrete Research*. 40 (2010) 77–84. <https://doi.org/10.1016/j.cemconres.2009.08.026>.
- [17] J. Yammine, M. Chaouche, M. Guerinnet, M. Moranville, N. Roussel, From ordinary rheology concrete to self compacting concrete: A transition between frictional and hydrodynamic interactions, *Cement and Concrete Research*. 38 (2008) 890–896.
- 695 [18] D. Marchon, S. Kawashima, H. Bessaies-Bey, S. Mantellato, S. Ng, Hydration and rheology control of concrete for digital fabrication: Potential admixtures and cement chemistry, *Cement and Concrete Research*. 112 (2018) 96–110.  
<https://doi.org/10.1016/j.cemconres.2018.05.014>.
- 700 [19] L. Reiter, T. Wangler, A. Anton, R.J. Flatt, Setting on demand for digital concrete – Principles, measurements, chemistry, validation, *Cement and Concrete Research*. 132 (2020) 106047.  
<https://doi.org/10.1016/j.cemconres.2020.106047>.

- 705 [20] L. Reiter, T. Wangler, N. Roussel, R.J. Flatt, The role of early age structural  
build-up in digital fabrication with concrete, *Cement and Concrete Research*.  
112 (2018) 86–95. <https://doi.org/10.1016/j.cemconres.2018.05.011>.
- [21] F. Bos, R. Wolfs, Z. Ahmed, T. Salet, Large Scale Testing of Digitally  
710 Fabricated Concrete (DFC) Elements, 2019. [https://doi.org/10.1007/978-3-319-99519-9\\_12](https://doi.org/10.1007/978-3-319-99519-9_12).
- [22] F. Bos, R. Wolfs, Z. Ahmed, T. Salet, Additive manufacturing of concrete in  
construction: potentials and challenges of 3D concrete printing, *Virtual and  
Physical Prototyping*. 11 (2016) 209–225.  
<https://doi.org/10.1080/17452759.2016.1209867>.
- 715 [23] L.K. Mettler, F.K. Wittel, R.J. Flatt, H.J. Herrmann, Evolution of strength and  
failure of SCC during early hydration, *Cement and Concrete Research*. 89  
(2016) 288–296. <https://doi.org/10.1016/j.cemconres.2016.09.004>.
- [24] J. Engmann, C. Servais, A.S. Burbidge, Squeeze flow theory and applications  
to rheometry: a review, *Journal of Non-Newtonian Fluid Mechanics*. 132  
720 (2005) 1–27.
- [25] N. Roussel, C. Lanos, Plastic fluid flow parameters identification using a  
simple squeezing test, *Applied Rheology*. 13 (2003) 132–139.
- [26] Z. Toutou, N. Roussel, C. Lanos, The squeezing test: a tool to identify firm  
cement-based material’s rheological behaviour and evaluate their extrusion  
725 ability, *Cement and Concrete Research*. 35 (2005) 1891–1899.
- [27] N. Roussel, P. Coussot, “Fifty-cent rheometer” for yield stress measurements:  
From slump to spreading flow, *Journal of Rheology*. 49 (2005) 705–718.  
<http://dx.doi.org/10.1122/1.1879041>.
- [28] N. Ducoulombier, P. Carneau, R. Mesnil, L. Demont, J.-F. Caron, N. Roussel,  
730 “The Slug Test”: Inline Assessment of Yield Stress for Extrusion-Based  
Additive Manufacturing, in: *RILEM International Conference on Concrete and  
Digital Fabrication*, Springer, 2020: pp. 216–224.
- [29] Y. Jacquet, V. Picandet, D. Rangeard, A. Perrot, Gravity Driven Tests to Assess  
Mechanical Properties of Printable Cement-Based Materials at Fresh State, in:  
735 *RILEM International Conference on Concrete and Digital Fabrication*,  
Springer, 2020: pp. 280–289.
- [30] S. Ma, Y. Qian, S. Kawashima, Experimental and modeling study on the non-  
linear structural build-up of fresh cement pastes incorporating viscosity  
modifying admixtures, *Cement and Concrete Research*. 108 (2018) 1–9.
- 740 [31] Y. Qian, S. Kawashima, Use of creep recovery protocol to measure static yield  
stress and structural rebuilding of fresh cement pastes, *Cement and Concrete  
Research*. 90 (2016) 73–79.
- [32] N. Roussel, H. Bessaies-Bey, S. Kawashima, D. Marchon, K. Vasilic, R. Wolfs,  
Recent advances on yield stress and elasticity of fresh cement-based materials,  
745 *Cement and Concrete Research*. 124 (2019) 105798.
- [33] N. Roussel, G. Ovarlez, S. Garrault, C. Brumaud, The origins of thixotropy of  
fresh cement pastes, *Cement and Concrete Research*. 42 (2012) 148–157.  
<http://dx.doi.org/10.1016/j.cemconres.2011.09.004>.
- 750 [34] B. Panda, J.H. Lim, M.J. Tan, Mechanical properties and deformation  
behaviour of early age concrete in the context of digital construction,  
*Composites Part B: Engineering*. 165 (2019) 563–571.

- 755 [35] T.T. Le, S.A. Austin, S. Lim, R.A. Buswell, A.G.F. Gibb, T. Thorpe, Mix design and fresh properties for high-performance printing concrete, *Materials and Structures*. 45 (2012) 1221–1232. <https://doi.org/10.1617/s11527-012-9828-z>.
- [36] A. Bouvet, E. Ghorbel, R. Bennacer, The mini-conical slump flow test: Analysis and numerical study, *Cement and Concrete Research*. 40 (2010) 1517–1523.
- 760 [37] J.E. Wallevik, Relationship between the Bingham parameters and slump, *Cement and Concrete Research*. 36 (2006) 1214–1221.
- [38] N. Roussel, Correlation between yield stress and slump: comparison between numerical simulations and concrete rheometers results, *Materials and Structures*. 39 (2006) 501.
- 765 [39] N. Roussel, C. Stéfani, R. Leroy, From mini-cone test to Abrams cone test: measurement of cement-based materials yield stress using slump tests, *Cement and Concrete Research*. 35 (2005) 817–822.
- [40] A. Perrot, D. Rangeard, N. Venkatesh, V. Mechtcherine, Extrusion of cement-based materials - an overview, *RILEMTechLett*. 3 (2019). <https://doi.org/10.21809/rilemtechlett.2018.75>.
- 770 [41] R.J. Flatt, P. Bowen, Yodel: a yield stress model for suspensions, *Journal of the American Ceramic Society*. 89 (2006) 1244–1256.
- [42] F. Mahaut, S. Mokéddem, X. Chateau, N. Roussel, G. Ovarlez, Effect of coarse particle volume fraction on the yield stress and thixotropy of cementitious materials, *Cement and Concrete Research*. 38 (2008) 1276–1285. <https://doi.org/10.1016/j.cemconres.2008.06.001>.
- 775 [43] R. Jayathilakage, P. Rajeev, J.G. Sanjayan, Yield stress criteria to assess the buildability of 3D concrete printing, *Construction and Building Materials*. 240 (2020) 117989.
- [44] B. Mazhoud, A. Perrot, V. Picandet, D. Rangeard, E. Courteille, Underwater 3D printing of cement-based mortar, *Construction and Building Materials*. 214 (2019) 458–467.
- 780 [45] T. Lecompte, A. Perrot, Non-linear modeling of yield stress increase due to SCC structural build-up at rest, *Cement and Concrete Research*. 92 (2017) 92–97. <https://doi.org/10.1016/j.cemconres.2016.11.020>.
- 785 [46] J. Kruger, S. Zeranka, G. van Zijl, 3D concrete printing: a lower bound analytical model for buildability performance quantification, *Automation in Construction*. 106 (2019) 102904.
- [47] S. Mantellato, M. Palacios, R.J. Flatt, Relating early hydration, specific surface and flow loss of cement pastes, *Materials and Structures*. 52 (2019) 5. <https://doi.org/10.1617/s11527-018-1304-y>.
- 790 [48] N. Roussel, A thixotropy model for fresh fluid concretes: Theory, validation and applications, *Cement and Concrete Research*. 36 (2006) 1797–1806. <http://dx.doi.org/10.1016/j.cemconres.2006.05.025>.
- [49] S. Mantellato, Flow loss in superplasticized cement pastes, ETH Zurich, 2017.
- 795